Journal of Photonics for Energy

PhotonicsforEnergy.SPIEDigitalLibrary.org

Temperature and current dependence of the magnetoresistive behavior of poly(styrene-sulfonate)-doped poly(3,4-ethylenedioxythiophene) (PEDOT:PSS)

Philippe Klemm
Sebastian Bange
Hans Malissa
Christoph Boehme
John M. Lupton

SPIE.

Philippe Klemm, Sebastian Bange, Hans Malissa, Christoph Boehme, John M. Lupton, "Temperature and current dependence of the magnetoresistive behavior of poly(styrene-sulfonate)-doped poly(3,4-ethylenedioxythiophene) (PEDOT:PSS)," *J. Photon. Energy* **8**(3), 032216 (2018), doi: 10.1117/1.JPE.8.032216.

Temperature and current dependence of the magnetoresistive behavior of poly(styrene-sulfonate)-doped poly(3,4-ethylenedioxythiophene) (PEDOT:PSS)

Philippe Klemm,[a] Sebastian Bange,[a] Hans Malissa,[a,b] Christoph Boehme,[b,*] and John M. Lupton[a,b]

[a]Universität Regensburg, Institut für Experimentelle und Angewandte Physik, Regensburg, Germany

[b]University of Utah, Department of Physics and Astronomy, Salt Lake City, Utah, United States

Abstract. We investigate the magnetic field effects in thin-film diodes made of the conducting polymer poly(styrene-sulfonate)-doped poly(3,4-ethylenedioxythiophene) as a function of temperature and electrical current. Magnetoresistance of these devices can be measured to high precision on two distinct magnetic field scales: <3 mT, where a pronounced nonmonotonic magnetoresistance response can be resolved, owing to weak hyperfine coupling, and at intermediate magnetic fields, ranging between 3 and 10 mT, where strong monotonic magnetoresistance is seen. The detailed examination of the magnetoresistance effects in both regimes allows one to scrutinize the accuracy of the underlying models for the behavior of these kinds of materials. [DOI: 10.1117/1.JPE.8.032216]

Keywords: organic semiconductors; conducting polymers; magnetoresistance; magnetic field effects; poly(styrene-sulfonate)-doped poly(3,4-ethylenedioxythiophene) (PEDOT:PSS).

Paper 18022SS received Feb. 8, 2018; accepted for publication Apr. 18, 2018; published online May 30, 2018.

1 Introduction

Spin-pair correlations within organic compounds continue to intrigue researchers at the intersection of biology, chemistry, and physics.[1–6] One approach to study spin-pair correlations is the use of magnetic fields of different strengths and the subsequent observation of changes of macroscopic properties of the objects of interest.[7–12] However, when investigating conducting polymers in a solid thin-film form, the examined materials are often incorporated in heterostructure devices consisting of multiple layers and mixtures of materials.[1,2,4,9,12,13] We have recently shown that the study of specific magnetic field effects, such as the ultrasmall magnetic field effect (<1 mT), may be hampered in these devices.[14] In heterostructures, magnetic field effects of different organic compounds can be superimposed, resulting in a difficult interpretation of results that can cause ambiguities with regard to the assignment of the physical mechanisms responsible for the observed behavior as well as their quantitative characteristics. Although a rather complex compound in itself, devices with an active layer consisting solely of the polymer poly(styrene-sulfonate)-doped poly(3,4-ethylenedioxythiophene) (PEDOT:PSS) exhibit a well-pronounced ultrasmall magnetic field effect in conductivity, owing to relatively weak hyperfine magnetic field effects compared to other conducting materials whose hyperfine fields are one- to two-orders higher in magnitude.[14] Therefore, a detailed investigation of the magnetoresistance of PEDOT:PSS on different magnetic field scales may provide the means to gain insights into

*Address all correspondence to: Christoph Boehme, E-mail: boehme@physics.utah.edu

the various mechanisms that have been proposed for the origin of polymer magnetoresistance in general.[1,15–18]

Here, we present a thorough examination of the temperature dependence as well as the electrical power dependence of the ultrasmall and intermediate magnetic field effects of a thin-film device with an active layer of PEDOT:PSS. We demonstrate that temperature changes on the order of a few degrees can have a distinct influence on the magnetoresistive response of PEDOT:PSS. In addition, magnetoresistance at 4.5 K is investigated in detail as a function of driving current ranging over four orders of magnitude, from 100 nA to 1 mA, and is found to exhibit a nonmonotonic behavior. Although the strength of the intermediate and the ultrasmall magnetic field effect do not correlate, remarkably, the overall width of the magnetoresistance curve and the position of the minimum of the ultrasmall magnetic field effect exhibit a linear correlation.

2 Experiments

Based on our previous study,[14] a 120-nm-thick layer of PEDOT:PSS (Heraeus Clevios P VP AI 4083) was spin-coated onto a prepatterned indium tin oxide (ITO)-covered glass substrate. An aluminum-top contact was thermally evaporated and defined, in conjunction with the ITO bottom contact, an active pixel area of 2.4 mm^2. Measurements were performed under a vacuum atmosphere (10^{-6} mbar) in a cold-finger cryostat, which provided temperature control between 4.5 K and room temperature. A single solenoid centered around the device under test provided the external magnetic field of up to 60 mT oriented normal to the sample plane. The samples were driven at constant current by a source measure unit. Changes in the resistance of the sample were monitored with a digital multimeter via a voltage measurement across the device. A detailed description of the measurement setup is also found in Ref. 14. The current–resistance characteristics of a single device in absence of an external magnetic field for multiple temperatures are shown in Fig. 1.

As previously reported, the PEDOT:PSS device retains ohmic behavior (i.e., a resistance independent of current) at room temperature up to driving currents of 300 μA and shows nonohmic behavior for higher driving currents.[14] The critical current for the transition of ohmic to nonohmic behavior decreases with temperature, down to 30 nA at 4.2 K. This crucial fact is often overlooked in temperature-dependent studies of multilayer devices employing PEDOT:PSS as a hole injection layer, but should not come as a surprise: as in every doped conductor, the number of free charges is temperature-dependent. The absolute resistance in the ohmic regime increases with decreasing temperature, as is expected of a highly doped polymer such as PEDOT:PSS.[19] The points at which the temperature- and power-dependent magnetoresistance measurements were performed are marked by circles.

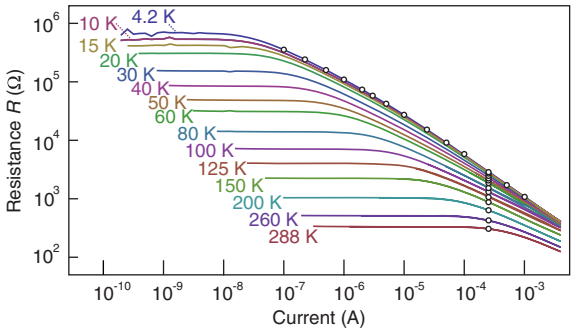

Fig. 1 Current–resistance characteristics of an ITO/PEDOT:PSS/aluminum thin-film device at different temperatures. Whereas at room temperature the behavior of the given device remains ohmic up to a driving current of 300 μA, at low temperature the onset of nonohmic behavior occurs at up to four orders of magnitude smaller currents. As a visual aid, the parameter points for the temperature and driving current-dependent magnetoresistance measurements shown in Figs. 2 and 3 are highlighted by circles.

3 Magnetoresistance Dependence on Temperature

The magnetoresistance measurements were carried out on the same setup and under the same measurement conditions as the current–resistance characteristics. As described in our previous studies,[14] the highest accuracy in measurement is achieved by taking multiple, consecutive magnetoresistance sweeps after settling times that are on the order of minutes at least. The resulting magnetoresistance measurements at a constant driving current of $I = 250\ \mu$A for multiple temperatures, marked in Fig. 1 by circles, are shown in Fig. 2(a). Here, the normalized magnetoresistance $\frac{\Delta R}{R} = \frac{R(B)-R(0)}{R(0)}$ is depicted versus the externally applied magnetic field, corrected for the geomagnetic field by shifting the curve along the field axis. As previously reported, data associated with the intermediate magnetic field effect, i.e., the magnetoresistance on the magnetic field scale 5 mT < $|B|$ < 60 mT, are well described by the empirical function $R(B) = \text{const.} + (\frac{B}{|B|+B_0})^2$. A clear anticorrelation between the magnitude of the maximally observed magnetoresistance and temperature is evident, with a magnitude of 630 ppm occurring at 4.2 K and a magnitude of 260 ppm being found at 288 K. To further analyze the response, we estimate the width of the measured curves by computing the full-width at half-maximum (FWHM) ΔB. Since the magnetoresistance does not saturate, the effective baseline for determining ΔB is dependent on the overall magnetic field range and therefore ΔB merely constitutes a rough estimate of the overall FWHM of the magnetoresponse. Nevertheless, we can use ΔB as a useful metric. The FWHM ΔB of the magnetoresistance traces is plotted in Fig. 2(b). An almost linear increase of ΔB from 4.8 to 8 mT is seen with the temperature increasing from 4.2 to 200 K. However, starting from 200 K, ΔB remains constant up to room temperature within the margin of error, even though 200 K is not a critical temperature in terms of the transition from

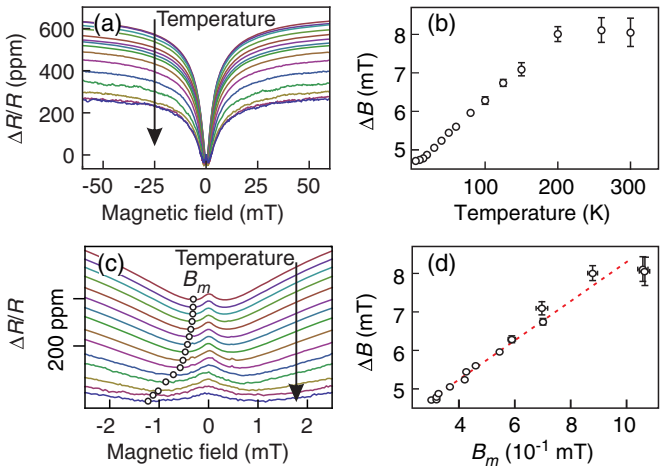

Fig. 2 Magnetoresistance of an ITO/PEDOT:PSS/aluminum thin-film device under a constant current of $I = 250\ \mu$A for temperatures between 288 and 4.5 K. Exact temperature steps are shown in Fig. 1. (a) Magnetoresistance measured up to an external magnetic field of 60 mT. Although the maximum magnetoresistance value and the FWHM of the curve change with the temperature, the intermediate-field magnetoresistance data in the intervals −60 to −5 mT and 5 to 60 mT are well described by the function $R(B) = \text{const.} + (\frac{B}{|B|+B_0})^2$. (b) FWHM of the measured magnetoresistance function with respect to the extreme values of the observed magnetoresistance. Note that this value is proportional but not identical to the FWHM of the entire magnetoresistance function. The FWHM of the measured magnetoresistance increases from 4.8 mT at 4.5 K almost linearly to 8 mT at 200 K, at which point it remains constant within the margin of error. (c) Data from (a) plotted on a smaller magnetic field range, showcasing the ultrasmall magnetic field effect at different temperatures. The data are shifted on the y axis to provide visual clarity, and the tics indicate the scale bar. As a guide to the eye, the magnetic field B_m is marked by circles, describing the minimum in the nonmonotonic magnetoresistance response. B_m increases monotonically as the temperature rises. (d) The FWHM associated with the intermediate magnetic field effect shown as a function of B_m. A direct correlation between these two phenomenological values is observed, even though they occur on very different magnetic field scales.

nonohmic to ohmic behavior of the current–resistance characteristics at 250 μA (cf. Fig. 1). The lack of significant changes of the intermediate magnetic field effect for this temperature range suggests that the current–resistance characteristics are not a defining factor for the magnetoresistance. To enable a closer look at the ultrasmall magnetic field effect, Fig. 2(c) shows a magnified view of the data where the individual magnetoresistance traces are offset on the vertical axis for visual clarity. The lowest observed magnetoresistance value, a phenomenological measure of the relevant field scale for the ultrasmall magnetic field effect, decreases from −26 ppm at 4.2 K to −50 ppm at 200 K. For higher temperatures, it reverses and reaches a value of −34 ppm at 288 K. The magnetic field $B_m(T)$ at which this minimum occurs is marked by black circles on the negative half of Fig. 2(b). A clear, monotonic increase of $B_m(T)$ from 300 μT at 4.2 K to 1050 μT at 288 K is observed. Interestingly, when the FWHM of the intermediate magnetic field effect ΔB is plotted as a function of $B_m(T)$ in Fig. 2(d), a clear linear relationship is observed. Since $B_m(T)$ and ΔB both result from the interplay of two most likely independent magnetic field effects of different widths (i.e., different magnetic field dependencies) and strengths, such a strong correlation is rather unexpected.

4 Magnetoresistance Dependence on the Device Operating Point (Current)

To complement the temperature-dependent data, magnetoresistance measurements were conducted as a function of the device current at a temperature of 4.5 K. In Fig. 3(a), the results of

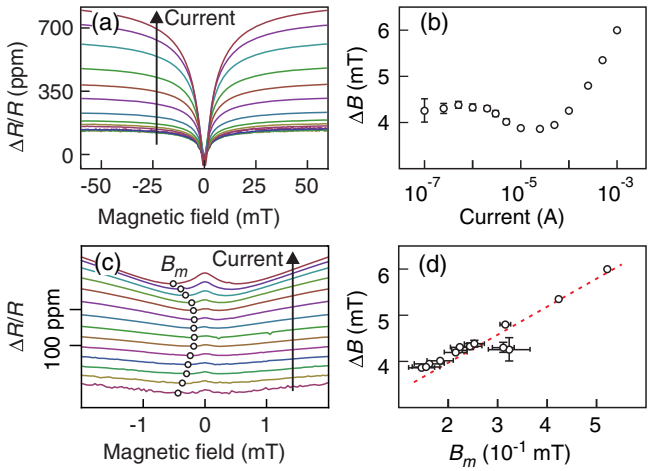

Fig. 3 Magnetoresistance of a PEDOT:PSS device at 4.5 K as a function of current ranging from 100 nA to 1 mA. The current steps are shown in Fig. 1. (a) Magnetoresistance measured up to an external magnetic field magnitude of 60 mT. As the driving current increases, the strength of the magnetoresistance reaches up to 800 ppm, but even at the lowest driving currents of 100 nA, the magnetoresistance is clearly discernible. As for the temperature-dependent measurements, the magnetoresistance data in the field interval from −60 to −5 mT and 5 to 60 mT are well described by the function $R(B) = \text{const.} + (\frac{B}{|B|+B_0})^2$. (b) Estimated FWHM ΔB evaluated from the maximum observed magnetoresistance. ΔB has a constant value of 4.3 mT for low driving currents from 100 nA to 2 μA. Upon increasing the driving current, ΔB drops down to 3.8 mT at 250 μA. As the driving current is increased even further, ΔB rises again up to 6 mT at 1 mA current. (c) A zoom into the ultrasmall magnetic field effect of a PEDOT:PSS device at 4.5 K. The data are offset on the vertical axis to provide visual clarity, with the tics providing a scale bar. As a guide to the eye, the magnetic fields B_m where the lowest magnetoresistance value occurs are marked by circles. Interestingly, a clear minimum in B_m develops for driving currents between 1 and 10 μA. The strength of the ultrasmall magnetic field effect is highly dependent on the applied current, and almost vanishes with a magnitude as low as 10 ppm at the lowest current. (d) Plot of the FWHM ΔB associated with the intermediate-strength magnetic field effect as a function of B_m, which describes the ultrasmall magnetic field effect. As with the temperature-dependent data, a linear relationship between these two observables is found.

these measurements are shown for currents identical to those used in Fig. 1. As for the temperature-dependent magnetoresistance measurements in Fig. 2, the current dependencies observed for the intermediate magnetic field regime (i.e., 5 mT < $|B|$ < 60 mT) are well described by the empirical function $f(B) = \text{const.} + (\frac{B}{|B|+B_0})^2$. The magnitude of the intermediate magnetic field effect of 140 ppm does not change between 100 nA and 1 μA. For higher driving currents, the magnitude increases up to 800 ppm at 1 mA. The corresponding FWHM ΔB of the intermediate magnetic field effect is shown in Fig. 3(b). In contrast to the temperature dependence of ΔB, the current dependence is far from monotonic. While ΔB is constant within the margin of error at 4.4 mT for currents between 100 nA and 2 μT, it starts to fall for higher currents. At 250 μA, a minimum value is reached and the FWHM is measured as 3.8 mT. As the current is increased further, ΔB increases again and reaches a value of 6 mT at the highest applied current of 1 mA. In Fig. 3(c), a zoom into the region of the ultrasmall magnetic field is shown, where the data points are offset on the vertical axis to aid visual clarity. The lowest observed magnetoresistance value is −20 ppm at 100 nA. An increase of the magnitude up to −8 ppm at 10 μT is followed by a decrease down to −62 ppm at 1 mA. As in the discussion of the temperature-dependent data, the magnetic field $B_m(I)$ at which this minimum occurs is marked as circles on the negative half of the plot. In contrast to the temperature-dependent measurements, however, the behavior becomes nonmonotonic. As for ΔB in the intermediate magnetic field range, $B_m(I)$ drops from 320 μT at 100 nA to a minimum of 150 μT at 250 μA and rises up to 520 μT at 1 mA again. Surprisingly, when $\Delta B(I)$ is plotted as a function of $B_m(I)$ as shown in Fig. 3(d), a linear relationship is found in the driving-current-dependent data, as in the temperature-dependent measurements. Both intermediate and ultrasmall magnetic field effects appear to be heavily affected by a change in driving current, which may indicate a strong dependence on the carrier density within the PEDOT:PSS thin-film diode. As the carrier density increases with increasing current, the average distance between individual charge carriers likely decreases. This change should influence the dipolar and exchange interaction strengths, which will impact the magnetic-field response.[20–22]

5 Discussion and Conclusions

To our knowledge, the experimental data presented above reflects the most comprehensive study of PEDOT:PSS magnetoresistance. It is consistent with previously reported behavior of magnetoresistance of PEDOT:PSS thin-film diodes,[14,23] and it reveals the full complexity of the PEDOT:PSS magnetoresistance due to its nontrivial dependence on the device operating point. Although it has been previously concluded that intermediate and ultrasmall magnetic field effects have to originate from different microscopic effects, given the strong differences in the evolution of the magnitude with magnetic field, the clear correlation of the FWHM of the intermediate magnetic field effect ΔB and the minimum of magnetoresistance attributed to the ultrasmall magnetic field effect B_m put the interpretation of magnetoresistance data based on these phenomenological characteristics in question. While in previous studies two models of magnetoresistance have been excluded as possible origins of magnetoresistance in PEDOT:PSS,[14] this study may provide the means necessary to analyze the validity of two other models: the spin precession model and electronic spin–spin interactions as the origin of organic magnetoresistance.[16,17,24] Future microscopic simulations should aim at replicating these complex functionalities as a function of temperature and driving current in order to scrutinize possible microscopic magnetic field dependencies.

Acknowledgments

This work was compiled on the occasion of Professor Z. Valy Vardeny's 70th birthday workshop. Professor Vardeny has made seminal contributions to both the discovery and exploration of magnetoresistance effects in organic semiconductors as well as to the development of a fundamental theoretical understanding. The authors thank Professor Vardeny for these groundbreaking contributions which, in many ways, restarted this research field,

merging spin chemistry with solid-state spintronics. The authors also express their sincere gratitude for many years of collaboration, support, stimulating discussions, and friendship. Financial support from the German Science Foundation through the SFB 1277 Project B03 is gratefully acknowledged.

References

1. T. D. Nguyen et al., "Magnetoconductance response in unipolar and bipolar organic diodes at ultrasmall fields," *Phys. Rev. Lett.* **105**(16), 166804 (2010).
2. T. D. Nguyen, E. Ehrenfreund, and Z. V. Vardeny, "Organic magneto-resistance at small magnetic fields: compass effect," *Org. Electron.* **14**(7), 1852–1855 (2013).
3. S. Engels et al., "Anthropogenic electromagnetic noise disrupts magnetic compass orientation in a migratory bird," *Nature* **509**(7500), 353–356 (2014).
4. D. Chaudhuri et al., "Metal-free OLED triplet emitters by side-stepping Kasha's rule," *Angew. Chem. Int. Ed.* **52**(50), 13449–13452 (2013).
5. W. J. Baker et al., "Robust absolute magnetometry with organic thin-film devices," *Nat. Commun.* **3**, 898 (2012).
6. S. L. Bayliss et al., "Geminate and nongeminate recombination of triplet excitons formed by singlet fission," *Phys. Rev. Lett.* **112**(23), 238701 (2014).
7. Z. H. Xiong et al., "Giant magnetoresistance in organic spin-valves," *Nature* **427**(6977), 821–824 (2004).
8. T. D. Nguyen et al., "Isotope effect in spin response of pi-conjugated polymer films and devices," *Nat. Mater.* **9**(4), 345–352 (2010).
9. Ö. Mermer et al., "Large magnetoresistance in nonmagnetic π-conjugated semiconductor thin film devices," *Phys. Rev. B* **72**(20), 205202 (2005).
10. O. Efimova and P. J. Hore, "Role of exchange and dipolar interactions in the radical pair model of the avian magnetic compass," *Biophys. J.* **94**(5), 1565–1574 (2008).
11. S. G. Boxer, C. E. D. Chidsey, and M. G. Roelofs, "Magnetic field effects on reaction yields in the solid state: an example from photosynthetic reaction centers," *Annu. Rev. Phys. Chem.* **34**(1), 389–417 (1983).
12. W. Ratzke et al., "Effect of conjugation pathway in metal-free room-temperature dual singlet-triplet emitters for organic light-emitting diodes," *J. Phys. Chem. Lett.* **7**(22), 4802–4808 (2016).
13. Y. Sheng et al., "Hyperfine interaction and magnetoresistance in organic semiconductors," *Phys. Rev. B* **74**(4), 045213 (2006).
14. P. Klemm et al., "Nanotesla magnetoresistance in π-conjugated polymer devices," *Phys. Rev. B* **95**(24), 241407 (2017).
15. T. D. Nguyen et al., "Isotope effect in the spin response of aluminum tris(8-hydroxyquinoline) based devices," *Phys. Rev. B* **85**(24), 245437 (2012).
16. A. Schellekens et al., "Microscopic modeling of magnetic-field effects on charge transport in organic semiconductors," *Phys. Rev. B* **84**(7), 075204 (2011).
17. N. J. Harmon and M. E. Flatté, "Effects of spin-spin interactions on magnetoresistance in disordered organic semiconductors," *Phys. Rev. B* **85**(24), 245213 (2012).
18. S. P. Kersten et al., "Magnetic-field dependence of the electroluminescence of organic light-emitting diodes: a competition between exciton formation and spin mixing," *Phys. Rev. Lett.* **106**(19), 197402 (2011).
19. A. Elschner et al., *PEDOT—Principles and Applications of an Intrinsically Conductive Polymer*, CRC Press, Boca Raton, Florida (2010).
20. A. R. O'Dea et al., "Influence of dipolar interactions on radical pair recombination reactions subject to weak magnetic fields," *J. Phys. Chem. A* **109**(5), 869–873 (2005).
21. L. Yang et al., "Theoretical investigation on thermal effect in organic semiconductors," *Org. Electron.* **23**, 39–43 (2015).
22. Y. L. Zhang, X. J. Liu, and Z. An, "Temperature dependence of polaron stability in conjugated polymers," *Europhys. Lett.* **111**(1), 17009 (2015).
23. G. Joshi et al., "High-field magnetoresistance of organic semiconductors," arXiv:1804.09297 [cond-mat.mes-hall].

24. W. Wagemans and B. Koopmans, "Spin transport and magnetoresistance in organic semiconductors," *Phys. Status Solidi* **248**(5), 1029–1041 (2011).

Philippe Klemm received his PhD in physics from the University of Regensburg and currently works on inductive sensors in the private sector. His main academic area of interest are physics of materials irregularly shaped on the nanometer scale, including effects such as spin permutronics in polymer materials and plasmonics of precious metal nanostructures. He was awarded the University Prize of the City of Regensburg for his work on dual fluorescent and phosphorescent OLEDs in 2014.

Sebastian Bange obtained his PhD in physics from the University of Potsdam, Germany in 2009. He worked as a postdoctoral fellow with Prof. Lupton in Utah before joining his group in Regensburg as an Akademischer Rat in 2010. His research interests include the excitonic and charge transport properties of organic electronic devices, as well as linear and nonlinear optical spectroscopy of organic and inorganic semiconductors and nanoplasmonic systems.

Hans Malissa studied at the Johannes Kepler University Linz, Austria, where he obtained his doctor's degree in 2007. In 2009, he moved to Princeton University for a postdoctoral appointment through an Erwin Schrödinger Fellowship. In 2012, he moved to the University of Utah as a postdoctoral fellow and was appointed as a research assistant professor in 2015. Since 2018, he has worked for the University of Utah and at the University of Regensburg, Germany.

Christoph Boehme graduated from Heidelberg University majoring in physics in 2000, received his PhD in physics from the University of Marburg in 2003, and worked thereafter as postdoc at the Hahn–Meitner–Institut Berlin. He joined the University of Utah in 2006 as an assistant professor of physics, worked as tenured associate professor from 2010 until 2013, and as a professor since 2013. His research is focused on spin-dependent electronic transitions in condensed matter.

John M. Lupton holds a chair in physics at the University of Regensburg and is a research professor at the University of Utah, having been a full professor previously. After studying physics at the University of Durham he held appointments in St. Andrews, MPI Mainz and LMU Munich. Distinctions include a Packard Fellowship, a Research Corporation Scialog award, and an ERC Starting Grant. His interests span single-molecule spectroscopy of π-conjugated macromolecules, spin physics of molecular materials, and the optics of semiconductor and metallic nanostructures.